

First edition
2013-03-15

**Optics and photonics — Wavefront
sensors for characterising optical
systems and optical components**

*Optique et photonique — Capteurs de front d'onde pour
caractérisation des systèmes optiques et des composants optiques*



Reference number
ISO/TR 16743:2013(E)



COPYRIGHT PROTECTED DOCUMENT

© ISO 2013

All rights reserved. Unless otherwise specified, no part of this publication may be reproduced or utilized otherwise in any form or by any means, electronic or mechanical, including photocopying, or posting on the internet or an intranet, without prior written permission. Permission can be requested from either ISO at the address below or ISO's member body in the country of the requester.

ISO copyright office
Case postale 56 • CH-1211 Geneva 20
Tel. + 41 22 749 01 11
Fax + 41 22 749 09 47
E-mail copyright@iso.org
Web www.iso.org

Published in Switzerland

Contents	Page
Foreword	iv
1 Scope	1
2 Introduction to wavefront sensing techniques	1
3 Foucault knife-edge test	2
3.1 The knife-edge test	2
3.2 Variations on the knife-edge test	3
3.3 Application of knife-edge test to diode lasers	3
3.4 The pyramid sensor	3
4 Screen testing	4
4.1 General	4
4.2 Hartmann test	4
4.3 The development of automated wavefront sensing	5
4.4 Shack-Hartmann test	6
4.5 Measurements with a Shack-Hartmann sensor	7
5 Wavefront curvature sensors	8
5.1 General	8
5.2 Wavefront curvature sensing and phase diversity techniques	8
5.3 Phase diversity wavefront sensor with diffraction grating	9
6 Wavefront sensing by interferometry	10
6.1 General	10
6.2 Self-referencing interferometry	11
6.3 Electronic detection and phase measurement	12
6.4 Shearing interferometry	12
6.5 Point-diffraction interferometers with error-free reference wavefronts	17
6.6 Lateral shearing and the Ronchi test	20
6.7 Lateral shearing with a double frequency grating	21
7 Summary of wavefront sensing methods	22
Bibliography	25

Foreword

ISO (the International Organization for Standardization) is a worldwide federation of national standards bodies (ISO member bodies). The work of preparing International Standards is normally carried out through ISO technical committees. Each member body interested in a subject for which a technical committee has been established has the right to be represented on that committee. International organizations, governmental and non-governmental, in liaison with ISO, also take part in the work. ISO collaborates closely with the International Electrotechnical Commission (IEC) on all matters of electrotechnical standardization.

International Standards are drafted in accordance with the rules given in the ISO/IEC Directives, Part 2.

The main task of technical committees is to prepare International Standards. Draft International Standards adopted by the technical committees are circulated to the member bodies for voting. Publication as an International Standard requires approval by at least 75 % of the member bodies casting a vote.

In exceptional circumstances, when a technical committee has collected data of a different kind from that which is normally published as an International Standard ("state of the art", for example), it may decide by a simple majority vote of its participating members to publish a Technical Report. A Technical Report is entirely informative in nature and does not have to be reviewed until the data it provides are considered to be no longer valid or useful.

Attention is drawn to the possibility that some of the elements of this document may be the subject of patent rights. ISO shall not be held responsible for identifying any or all such patent rights.

ISO/TR 16743 was prepared by Technical Committee ISO/TC 172, *Optics and photonics*, Subcommittee SC 1, *Fundamental standards*.

Optics and photonics — Wavefront sensors for characterising optical systems and optical components

1 Scope

This Technical Report gives terms and definitions and describes techniques for the characterization of wavefronts influenced by optical systems and optical components. It describes basic configurations for a variety of wavefront sensing systems and discusses the usefulness of tests in different situations.

The aim is to cover practical instruments and techniques for measuring the wavefronts produced by optical systems and optical components. This Technical Report includes various implementations of the Hartmann method, the curvature sensor and applications of the knife-edge method. The use of interferometers is discussed. This Technical Report also includes techniques such as phase diversity and pyramid sensors, currently used in astronomy and being developed for other areas.

NOTE More information on interferometry can be found in ISO/TR 14999-1, ISO/TR 14999-2 and ISO/TR 14999-3.

This Technical Report explains briefly how these techniques work and includes diagrams illustrating the use of this type of equipment for making the measurements required for ISO 10110-5, ISO 10110-8, ISO 10110-12 (slope requirements) and ISO 10110-14.

2 Introduction to wavefront sensing techniques

Interferometry is a well-established technique for comparing a test wavefront with a reference wavefront, usually spherical or planar, and requires a degree of coherence between the two wavefronts to produce an interference pattern. Some interferometers for wavefront characterization are self-referencing, such as shearing interferometers. These reveal the slope of the wavefront at various points with values deduced from the interferogram and integrated to calculate the phase profile.

More recently non-interferometric techniques have been developed, partly driven by the needs of adaptive optics, and it is possible to apply these to wavefronts with limited coherence. The majority of these techniques are based on measuring the wavefront slope values.

Many of the non-interferometric techniques can be categorized as screen tests. A screen test is a general term for the test of a beam with an opaque plate placed or moved in the focusing beam and the irradiance pattern transmitted by the opaque plate analysed. The screen may have one or more holes, slits or edges to transmit part of the beam while blocking with the opaque part.

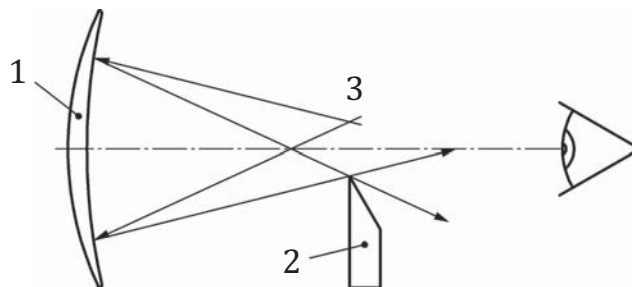
Non-interferometric techniques include focused waist (image of source) measurements and wavefront sampling which gives slope measurements. The knife-edge is a simple test that isolates regions of the wavefront to reveal aberrations. The Hartmann test uses a perforated screen to isolate bundles of rays and the direction of these bundles is measured to calculate the wavefront slopes. The Shack-Hartmann test uses an array of small lenses to sample the wavefront. The wavefront slopes are deduced from the positions of the focal spots generated by the lens array and the slope values are integrated to calculate the phase profile.

Wavefront curvature sensing and phase diversity techniques are a class of wavefront retrieval mechanisms that infer the wavefront from measurements of the intensity of the light as the beam propagates. Typically this involves the measurement of two images along the beam path, from which the intensity gradient is derived. Two standard approaches are to measure the intensity either side of a focus or either side of a pupil plane in an optical system. Phase diversity techniques use calculation algorithms for the retrieval of wavefront phase. Once the intensity data are collected, a processing step is required to calculate the wavefront. This can be achieved using the intensity transport equation,

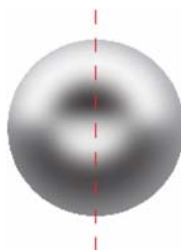
and solved by direct integration or iteratively using Fourier transform techniques.[11] Phase diversity methods are finding more use with faster phase retrieval methods as computation speeds increase.

3 Foucault knife-edge test

3.1 The knife-edge test



a) Test set-up



b) typical intensity pattern seen by observer

Key

- 1 mirror
- 2 knife-edge
- 3 source

Figure 1 — Knife-edge test for wavefront from a concave mirror

The knife-edge test is one of a family of techniques in which elements of a deformed wavefront are detected by blocking with an opaque mask that has an edge that clearly defines the boundary between the opaque and transmitting regions of the mask. The mask is placed in the plane of best focus of the wavefront.

The knife-edge test was reported by Foucault in 1858 as a method for examining the form of a concave mirror surface.[12] The mirror is used to form an off-axis image of a pinhole source placed in a plane containing the centre of curvature of the mirror and a blade with a knife-edge as shown in [Figure 1a](#)). The mirror is observed from the vicinity of the image and the knife-edge is moved across the line of sight until a shadow is seen to cross the mirror. The direction of movement of the shadow will depend on whether the image is formed in front of or behind the knife-edge. If the centre of curvature lies exactly in the plane of the pinhole and the knife-edge, the whole aperture of the mirror will darken simultaneously revealing imperfections in the image. When the knife-edge is scanned across, imperfections in the image will be revealed as dark and bright regions, simulated in [Figure 1b](#)).

Knife-edge scanning is a relatively simple method for measuring spot sizes but inaccuracies can occur due to uncertainties in the location of the knife-edge. The method has been applied to the measurement of spot diameters to a precision of better than 50 nm using interferometry to monitor the knife-edge

position.[13] In applications such as optical data recording, the size and structure of the smallest possible focused spot is important. These parameters are described by the point-spread function, a measure of the quality of the optical system.[14-16]

3.2 Variations on the knife-edge test

The Foucault knife-edge test can be used to make precise measurements of zonal errors in near-spherical wavefronts and is useful as a null test.[17] It is not, however, so useful for testing aspherical wavefronts.

The asymmetry of the single knife-edge allows systematic errors to accrue. A better arrangement is to use two knife-edges that block the light simultaneously in opposite directions. Either a thin wire or a thin slit will achieve this. A thin wire blocks out a very narrow region of the wavefront and the shadow patterns consist of thin dark contours. Platzcek and Gaviola applied the thin-wire method to the testing of parabolic mirrors.[18] They measured the caustic, which is the line of centres of curvature of the surface elements.

3.3 Application of knife-edge test to diode lasers

The characteristics of diode laser sources are dependent on the choice of semiconductor materials and the geometry of the junction structure. The active layer of a typical laser is about one tenth of a wavelength thick while the waveguide dimensions are typically 1 μm by 3 μm in the planes perpendicular and parallel to the junction respectively. Mode confinement is achieved either by gain guiding or by index guiding. A laser beam is emitted from the facet and diverges strongly due to the small size of the source.

Diffraction causes the beam to spread over large angles, typically ranging from 25° to 60° in the perpendicular direction and 7° to 35° in the junction plane. The radiation pattern is asymmetrical. Depending on the type of diode the mechanisms of constraining the beam in the plane of the active laser and in the plane normal to it are quite different and the wavefront becomes strongly astigmatic. The window in the canister containing the diode source is usually a thin plate and this can introduce spherical aberration. Anamorphic lenses are sometimes used to collimate the elliptical beam.[19,20] Near-field and far-field measurements are often required to fully characterize a laser diode.[21]

Knife-edge scanning is often recommended for the measurement of the astigmatic distance of wavefronts from diode lasers. The diode source is imaged at the plane of the knife edge with a relay lens such as a microscope objective. The total optical power passing the knife edge is measured with a photodiode and meter. This is plotted against knife edge position and an integrated power profile drawn. Differentiation of this curve gives the actual power profile from which the beam diameter, defined as full width at half maximum height, can be determined.

A beam diameter profile is produced by measuring the beam diameter at different points along the axis, achieved by displacing the source. The beam diameter profile is produced for movement of the knife edge in the direction perpendicular to the junction plane of the laser diode and the other for travel parallel to the junction plane. The astigmatic distance is defined as the displacement of the source between the minima of these plots.

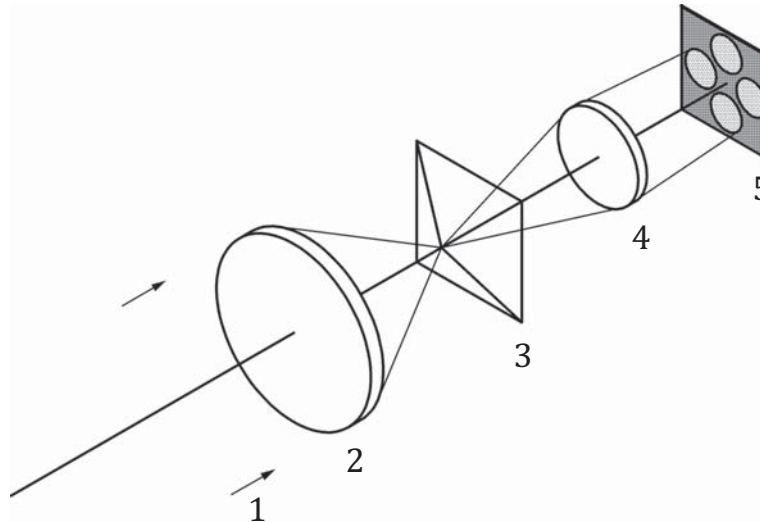
An advantage is that it is a simple test with no demands on coherence properties of source. It is sensitive to small deviations in slope of the sampled wavefront or to slope deviations that are changing slightly in magnitude or direction.

3.4 The pyramid sensor

The pyramid sensor may be considered as an extension of the knife-edge test and was primarily developed as a wavefront gradient sensor for astronomy.[22] In that application it uses a shallow glass pyramid with four faces, placed in the focal plane of a telescope and with the tip in line with the optical axis. An incident wavefront is collected by the telescope and focused to the pyramid which generates four beams, as shown in Figure 2. Another lens collects this light to reimage the telescope aperture and form four images on a detector array. The relative intensities of the light in these four images are compared and the wavefront gradients in two orthogonal directions are calculated. By modulating the position of the pyramid a linear gradient signal may be obtained. The accuracy of the pyramid sensor has

been investigated and the linearity considered from both the geometrical optical model and diffraction calculations.[23,24]

The test makes efficient use of the light and is able to sense two orthogonal directions. The main use of the pyramid sensor is with adaptive optics in astronomical and ophthalmic applications but its use is gradually being extended to more general wavefront sensing.



Key

- 1 wavefront
- 2 lens
- 3 pyramid prism
- 4 field lens
- 5 four images of entrance pupil on detector array

Figure 2 — Pyramid prism sensor

4 Screen testing

4.1 General

The Hartmann principle is based on a subdivision of the beam into a number of beamlets. This is either accomplished by an opaque screen with pinholes placed on a regular grid as in the Hartmann sensor or by a lenslet or microlens array as in the Shack-Hartmann sensor. The use of these techniques to determine the shape of a laser beam wavefront is described in ISO 15367-2. The techniques are also suitable for the measurement of non-laser wavefronts with reduced spatial coherence.

4.2 Hartmann test

The Hartmann test is based on a geometrical optics approach and uses a perforated screen or mask with multiple holes to sample the wavefront at a number of locations in a predetermined fashion.[25] The Hartmann test is often used for testing optical components such as telescope mirrors.[26]

The principle is that a portion of the wavefront, when tilted relative to an ideal wavefront in that region, causes light to come to a focus at a place other than the intended focus, or to intercept a chosen plane at

a location other than the one which would be obtained with light coming from the ideal wavefront and from that region.

The converse can be used to determine the tilt error in a portion of a wavefront, by determining where the light from that region intercepts a chosen plane, and what difference there is between that intersection and the one to be expected from a perfect wavefront.

With interferometry, deviations of the wavefront are found using the interference of light from two different regions. With screen testing, the light from each of the various regions of the wavefront is recorded on a photosensitive material, such as a photographic plate, which is measured after processing. The beam deviations are measured to obtain a surface slope error at the sampled points.

One of the major difficulties in screen testing is the introduction of errors through the method used to reduce the data in order to obtain the surface deviations. The main assumption is that the wavefront changes between samples are gradual rather than abrupt. Abrupt changes can be readily detected by other means such as the Foucault knife-edge test. The screen test is better suited for smooth wavefronts.

Several screens have been designed for testing including the Hartmann radial pattern. The holes in the screen have to be accurately placed and small but not so small that their diffraction images overlap at the recording stage.

The advantages of this test include the low number of components and low requirements for source coherence.

Disadvantages include:

- a) the Hartmann test samples the wavefront at a discrete number of points;
- b) the highest accuracy is achieved for the smoothest wavefronts;
- c) considerable time is required to record, process and measure the images on the photographic plate.

The main advantages of the Hartmann technique are:

- 1) wide dynamic range;
- 2) high optical efficiency;
- 3) suitability for partially coherent beams;
- 4) no requirement of spectral purity;
- 5) no ambiguity with respect to increment in phase angle.

Kingslake considered using the Hartmann test to measure spherical aberration in microscope objectives. A relatively small screen was needed and he realized that interference effects between the light transmitted by adjacent holes in the screen would be a problem. He therefore devised a method that used a single hole, traversed across the aperture to isolate a series of light beams in succession.^[27]

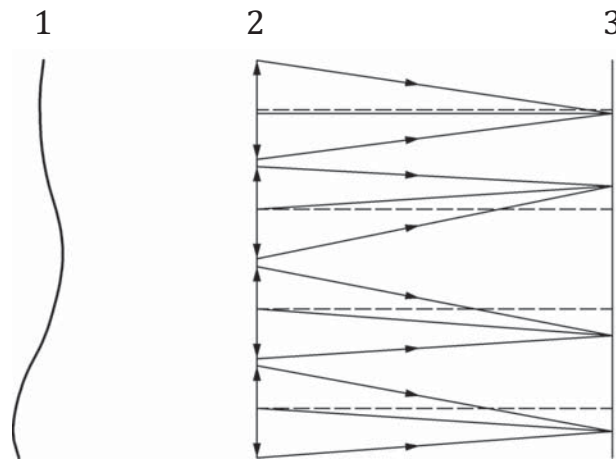
4.3 The development of automated wavefront sensing

In the Hartmann test a spot diagram is generated by the intersection of a defined plane and the ray bundles generated by a mask with an array of apertures. An automated device for achieving this was described by Baker and Whyte in 1964.^[28] They used a rotating polygon mirror to scan the pupil of the optical element under test. In a modified version a spiral disc scanner was used instead of the polygon mirror.^[29] The position at which each ray intersected the image plane was measured with a position-sensitive photodiode and the results displayed in real time on a cathode ray tube. A silicon quadrant detector was also used to measure the ray intersection coordinates. In a further development the system was able to measure wavefront aberration.^[30] In 1972 Williams described a system that measured both spot diagrams and wavefront aberrations using an image dissector tube as detector.^[31] The subsequent availability of large detector arrays and powerful portable computers has led to the development of equipment that operates on these principles and offers a serious alternative to the interferometers more

commonly found in optical workshops. One particularly successful configuration has been that due to Shack and Platt and described below.^[32]

4.4 Shack-Hartmann test

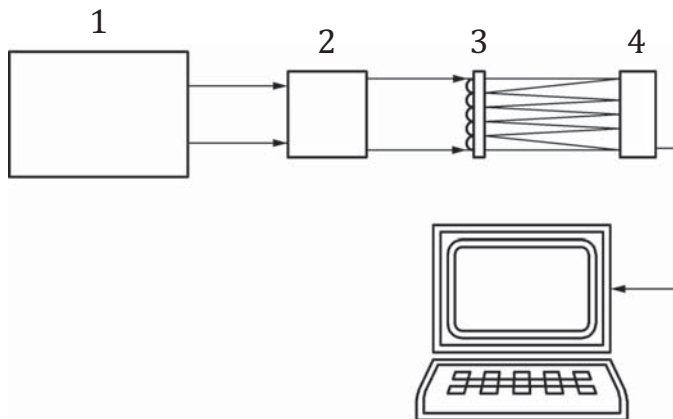
The Shack-Hartmann sensor uses an array of lenslets or microlenses to sample the wavefront.^[33] Compared with the Hartmann screen test this gives a better optical efficiency and in comparison with the automated system described above, the static lenslet array obviates the need to scan a pencil of light over the pupil of the test piece to sample the wavefront.



Key

- 1 wavefront
- 2 lenslet array
- 3 detector array

Figure 3 — Array of lenslets (microlenses) used to sample an incident wavefront



Key

- 1 source of wavefront
- 2 beam expansion or compression optics
- 3 lenslet array
- 4 detector array

Figure 4 — Experimental arrangement for wavefront measurement using Shack-Hartmann technique

The lenslet array divides the incident wavefront into a number of small areas, each of which is focused to a spot as in [Figure 3](#). If a plane reference wavefront is used at normal incidence the spots are formed on the lens axes. If the test wavefront is non-planar the spots are formed away from the axes. A charge-coupled device (CCD) is commonly used to capture the images of the multiple spots allowing the positions of the centroids of the spots to be determined. The transverse positions of the spots are related to the local slopes of the wavefront in the regions of the lens apertures and the form of the wavefront can be calculated using a small computer and dedicated software. In practice it is usually necessary to expand or contract the dimensions of the wavefront to match the dimensions of the lenslet and CCD arrays, as shown in the schematic layout in [Figure 4](#).

The average slope of each area of the wavefront that is sampled is determined from the focal length of each lens and the displacement of each image on the array relative to its position when a perfect test wavefront is used. The wavefront is computed from the slope data.

The method yields values for the local wavefront slopes. Two approaches, the zonal method and the modal method, can be used to fit the data to compute the wavefront. The choice depends on whether the estimate is a phase value in a local zone or a coefficient of an aperture function. In either case, the least squares method may be used for the phase reconstruction.^[34]

The Shack-Hartmann test can achieve a high sensitivity and is commonly used with adaptive optic systems where a deformable mirror is adjusted to give an optimum shape wavefront.^[35] The test has been applied to the measurement of wavefronts from diode lasers and to industrial infrared lasers. Michau et al. describe testing a collimated beam from a laser diode for space communication.^[36] One advantage of the Shack-Hartmann test is that the system is relatively simple with few components and can be used with low coherence wavefronts. Another advantage is the speed of the measurement. By use of the CCD and software to analyse the spot positions, the wavefront error is determined immediately. This measurement can then be used in the feedback controls of adaptive optics.

Disadvantages include the fact that the local wavefront is determined from the slope averaged over the lenslet aperture. The lateral resolution of the wavefront is limited by the pitch of the lenslets in the array. Wavefront measurement accuracy is limited by the accuracy with which the centroids of the focused spots can be determined.

4.5 Measurements with a Shack-Hartmann sensor

4.5.1 General

There are several Shack-Hartmann systems that are commercially available and each will come with its own instructions for use. Some common aspects include those described in [4.5.2](#) to [4.5.5](#).

4.5.2 Wavefront dynamic range

The wavefront shape must lie within the dynamic range of the sensor. The dynamic range depends primarily on the geometry of the lens array, for example lenses of longer focal length produce greater lateral displacement of the spots for a given angular tilt of wavefront. This limits the angular range that can be detected because the spot from one lens translates to a region of the detector assigned to an adjacent lens. However manufacturers have evolved different techniques for identifying and tracking the spots and thus extending the dynamic range.

4.5.3 Alignment

To make the most of the dynamic range the sensor must be carefully aligned. It is usually best to fit the sensor head to a precision adjustable tip/tilt table. The sensor should be aligned to be normal to the incident beam. One manufacturer recommends placing an adjustable aperture in the beam to define a small area and placing a small plane mirror on the sensor. The sensor is then tilted until the spot transmitted by the aperture is reflected back on itself. If this procedure is not possible and it is necessary to use the sensor in an off-normal position then the normal incidence calibration may not apply and a new reference measurement should be taken.

4.5.4 Illumination levels

The level of illumination reaching the sensor must be adjusted to within the limits of the sensor. Modern sensors have software that shows the signal levels along with minimum, maximum and average values.

The irradiance level can be adjusted by inserting neutral density filters in front of the camera but if the filters are not of high quality they may introduce additional aberrations to the wavefront. In that case a reference measurement should be made with the filter in place and the measured aberrations subtracted from the test wavefront results.

Another way of ensuring the light levels are within limits is to adjust the camera gain and exposure time. Typically, a value of 80 % of the maximum enables accurate measurements to be made without the danger of saturating the sensor. Changing the camera gain may change the signal to noise ratio.

4.5.5 Calibration

4.5.5.1 General

The calibration of the system should be checked before making a measurement. Some manufacturers will supply a data file from a calibration check made beforehand. Alternatively a live check may be performed by illuminating with a wavefront of known form such as a spherical or plane wavefront to provide an absolute calibration. Where it is only required to monitor the change in a wavefront, a measurement may be made before and after the change without necessarily carrying out an absolute calibration.

4.5.5.2 Calibrating sphericity component

The performance of the sensor in measuring spherical wavefronts of different radii can be assessed by monitoring a wavefront emitted by a point source such as an optical fibre and making measurements at different distances from the source. It is desirable to use a very long precision slideway for this.[\[37\]](#)

5 Wavefront curvature sensors

5.1 General

Wavefront curvature sensing is a technique which uses local tilt values to calculate wavefront curvature and commonly finds applications with adaptive optics. It measures the local wavefront curvature, together with the wavefront tilts at the aperture perpendicular to the edge in a direction perpendicular to the edge. A curvature sensor shown in [Figure 5](#) consists of two image detectors which detect the irradiance distributions either side of the wavefront focus produced by the action of lens L on the wavefront W.[\[38\]](#)

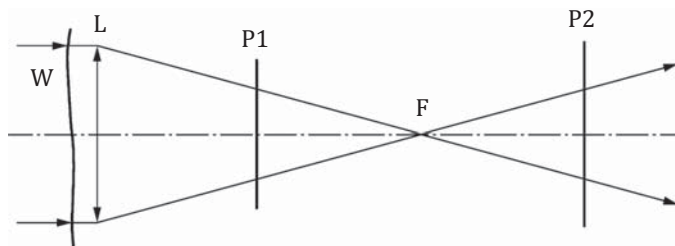


Figure 5 — Curvature sensing by measuring irradiance distributions either side of the focus

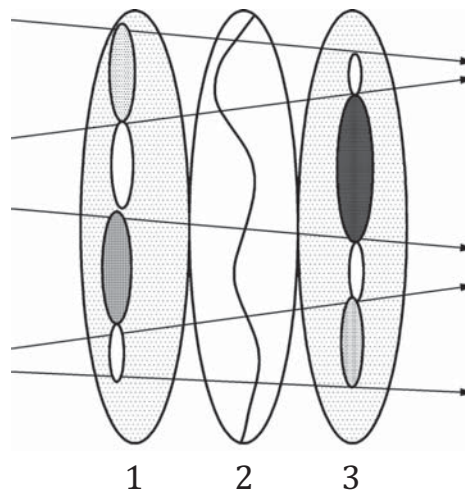
5.2 Wavefront curvature sensing and phase diversity techniques

Phase diversity techniques are a class of wavefront retrieval mechanisms that infer the wavefront from measurements of the intensity of the light as the beam propagates. Typically this involves the measurement of two images along the beam path, from which the intensity gradient is derived. Two

standard methods involve measuring the intensity either side of a focus as shown in [Figure 5](#) or either side of a pupil plane in an optical system. There are several techniques for imaging these planes onto a detector, including the use of a number of detectors, a dynamic mirror that changes focal length over time which is then synchronised to measurement on a detector, or a diffraction grating with optical power that images both measurement planes onto the same detector. The diffraction grating resembles the off-axis structure of a Fresnel zone plate and its use is described later in this Technical Report.

The curvature sensor shown in [Figure 5](#) consists of two detectors which detect the irradiance distributions in planes P1 and P2, either side of the wavefront focus F. The difference divided by the sum of the intensities of the two images at each position of the beam provides the curvature at that position. The sign of the calculation at the edge of the beam yields the slope of the wavefront compared to the reference spherical wavefront.

In [Figure 6](#) plane B may represent an input pupil plane in an optical system or simply a plane designated for wavefront characterization. The difference between the intensities in the images recorded when focused on plane A and plane C, divided by the sum of those intensities, provides an estimation of the rate of change of the intensity as the wavefront propagates (the axial intensity derivative). This derivative can be used to estimate the local wavefront curvature, indicated in [Figure 6](#) by the curved line in plane B, using a differential equation known as the Intensity Transport Equation, or ITE. Shrinkages of the illuminated region at the boundaries provide estimates of the wavefront slope around the boundary, which give the boundary conditions to use when solving the ITE.



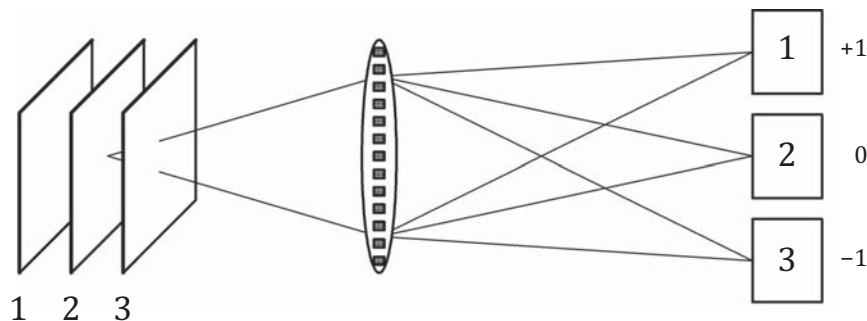
Key

- 1 plane A
- 2 plane B
- 3 plane C

Figure 6 — Curvature sensing by measuring irradiance in successive planes

5.3 Phase diversity wavefront sensor with diffraction grating

A recent development in wavefront sensing uses a special diffraction grating that resembles the off-axis structure of a Fresnel zone plate. The grating images planes on either side of an input pupil plane and, because the images are laterally separated, they can be recorded simultaneously with a single camera as shown in [Figure 7](#)^[39] Phase diversity algorithms are used to retrieve the wavefront phase from two images symmetrically placed about the wavefront to be reconstructed, and normal to the axis of propagation.^[40-43] From the wavefront phase of the two images, the wavefront at plane B is calculated.



Key

- 1 plane A
- 2 plane B
- 3 plane C

Figure 7 — Wavefront sampling with a special diffraction grating

If the images are captured about the system input pupil, this is essentially the same as a wavefront curvature algorithm where the measured intensity is directly related to the wavefront shape. By determining the wavefront shape, the location, direction and magnitude of the wavefront error can be calculated. This information can then be used to drive a corrective element in an adaptive optics system.

Hall et al. report a comparison of measurements made with a prototype instrument that used a cross-distorted diffraction grating. The wavefront measuring capability of the instrument was used to derive the beam propagation factor, $M2$, which is an important parameter for characterizing optical beams.^[44]

6 Wavefront sensing by interferometry

6.1 General

Interferometry is a widely used technique for analysing the shape of optical wavefronts and deducing information about the source of a wavefront and any optical components the wavefront may have traversed.

ISO/TR 14999-1 describes interferometric techniques commonly used for the purpose of characterizing the quality of optical components. The techniques covered include Newton, Fizeau, Haidinger, Mach-Zehnder and Twyman-Green interferometers. In these interferometers the wavefront returning from the item under test is compared to a reference wavefront generated by reflection at a reference surface, usually a partially reflecting plane or spherical surface manufactured to a high degree of precision and placed between the source and the surface under test. A range of methods for combining the test and reference wavefronts have been evolved for different types of interferometers and these include, for example, scatterplates which split wavefronts by optical scattering, gratings which operate by diffraction and birefringence prisms which operate by double refraction.

The techniques described above are used where it is possible to intercept the wavefront before it illuminates the surface under test and generate a reference wavefront. In another technique known as shearing interferometry the reference wavefront is a replica of, and can be generated from, the wavefront under test. The two wavefronts are given a relative displacement either in a transverse or radial sense, to generate an interference pattern from which the shape of the wavefront under test is calculated. In some designs of interferometer the reference wavefront is formed by expanding such a small portion of the test wavefront that the reference wavefront may be considered to be purely spherical.

The analysis of the phase profile of an optical wavefront is a task that is routinely encountered in metrology of optical components. The component under test is placed in the path of a test wavefront and the phase variations that are introduced are examined by interferometry. Some interferometric techniques assume that a coherent reference wavefront of simple form is readily available, others require a reference wavefront to be generated from the test wavefront.

Two self-referencing techniques are used to generate a reference wavefront from the test wavefront:

- a) a small portion of the test wavefront is selected and expanded to give a spherical reference wave;
- b) a replica of the entire wavefront is generated and compared to the test wavefront by shearing interferometry.

The first method treats the selected portion as being relatively unaberrated. This is expanded to compare with the aberrated test wavefront. The second method means that the aberrated wave is compared with an identical reference wave. By shearing the wavefronts, path differences are generated that enable the wavefront shapes to be determined. The wavefronts can be inverted, rotated and displaced in a variety of ways for comparison, depending on the information that is required to be extracted.

6.2 Self-referencing interferometry

This subclause considers the analysis of an isolated wavefront and assumes that a separate reference beam is not available. Self-referencing interferometers can be classified according to:

- a) the shearing geometry (the relation between the test and reference beams);
- b) the design layout (optical routes or beam paths);
- c) the method of beamsplitting.

The shearing geometry describes the generation and orientation of the reference beam and includes:

- 1) Lateral shear. This is obtained by displacing a copy of the wavefront laterally.
- 2) Reverse shear. Obtained by reversing a copy of the wavefront and superposing.
- 3) Inverted shear. Obtained by folding one part of the wavefront onto the other.
- 4) Radial shear. This is obtained by expanding or contracting a copy of the wavefront.
- 5) Large radial (exploded) shear. The copy wavefront is greatly expanded.
- 6) Point diffraction (error-free reference).

Beamsplitting can be achieved as follows:

- wavefront division - by division of area;
- amplitude division - by partial reflection;
- amplitude division - by diffraction.

The reference and test wavefronts may follow a common path on-axis or follow separate paths, as for example in the Mach-Zehnder design.

6.3 Electronic detection and phase measurement

Electronic phase measurement techniques enable interference patterns to be processed to a high degree of accuracy, ignoring noise generated by intensity variations that are not directly associated with the main interference pattern. Two general categories of phase measurement exist.

- a) Heterodyne or AC interferometry. The phase difference between two interfering beams is changed at a constant rate by producing a frequency difference between the two beams.
- b) Phase shifting or phase stepping. The phase difference between interfering beams is changed either by stepping a piezoelectric translator (PZT) pushing a mirror or by ramping the PZT to push the mirror as the detector array is integrating. The former is known as phase stepping and the latter as the integrating-bucket technique. The latter is faster.

Some of the interferometers described in this Technical Report are more readily adapted to electronic phase measurement than others. In many designs it is the detector that limits the range of wavelengths over which the interferometer can be used. The spatial geometry of the interference pattern must be known accurately and it is usual to use a charge coupled array (CCD) to detect the pattern. The wavelength range is limited by the spectral sensitivity of the CCD.

6.4 Shearing interferometry

6.4.1 General outline

The advantages of wavefront shearing interferometry were pointed out by Bates in 1946.^[45] He reported that the asphericity of an optical wavefront could be measured by testing it against itself with lateral displacement or shear. There was no need for an error-free wavefront to act as a reference standard. Different categories of shear include radial shear, rotational shear and reversal shear, the geometries being evident from the category name. Saunders introduced the concept of the inverting interferometer.^[46]

In the days before laser sources were invented, path lengths in interferometers had to be closely matched to retain coherence between the reference and test wavefronts. These often followed long and separate paths, rendering the test sensitive to environmental disturbances. The development of shearing interferometry reduced these restrictions and increased the ease of testing components such as large spherical and non-spherical mirrors.^[47,48]

When two wavefronts containing identical asphericities are exactly overlapped, a single bright fringe will cover the field of view. If a tilt is applied between the wavefronts, straight fringes parallel to the intersection of the wavefronts will result. When two wavefronts are sheared, an interferogram representing the difference between the two wavefronts will be obtained in the region of overlap and the interferogram reveals directly the slope of the wavefront. This is particularly true for small values of shear but becomes less exact for larger shears. Because the sensitivity of the test decreases as the magnitude of the shear decreases, the latter has to be carefully chosen and a compromise made between sensitivity and ease of interpretation. When the aberrated wavefront does not have circular symmetry the direction of shear is also important.

The asphericity revealed in the shearing interferogram will not be the same as that in the original wavefront but will depend upon it in a precise way. This is shown by expressing the wavefront under test by the polynomial expression.

$$w(x, y) = A_2(x^2 + y^2) + A_4(x^2 + y^2)^2 + A_6(x^2 + y^2)^3 + \dots$$

where x and y represent the coordinates of points on the wavefront. The aberrated wavefront is divided and sheared to form two interfering wavefronts, centred at C_1 and C_2 where $C_1 - C_2 = \Delta x$. Their combination centred at C can be written:

$$W_c(x, y) = A_2 \left[\left(x + \frac{\Delta x}{2} \right)^2 + y^2 \right] - A_2 \left[\left(x - \frac{\Delta x}{2} \right)^2 + y^2 \right]$$

$$\begin{aligned}
 &+A_4 \left[\left(x + \frac{\Delta x}{2} \right)^2 + y^2 \right]^2 - A_4 \left[\left(x - \frac{\Delta x}{2} \right)^2 + y^2 \right]^2 \\
 &+A_6 \left[\left(x + \frac{\Delta x}{2} \right)^2 + y^2 \right]^3 - A_6 \left[\left(x - \frac{\Delta x}{2} \right)^2 + y^2 \right]^3 + \dots
 \end{aligned}$$

Rearranging and, for small shears, neglecting Δx^3 , Δx^5 and higher orders,

$$W_c(x, y) = A_2 2x\Delta x + A_4 4x\Delta x(x^2 + y^2) + A_6 6x\Delta x(x^2 + y^2)^2 + \dots$$

A similar result can be obtained by differentiating the original wavefront equation. Therefore for small shears the shearing interferogram is equivalent to the differential of the equivalent Twyman-Green interferogram. For example if two wavefronts containing identical first order coma are sheared, then the fringe pattern in the overlap region contains change of focus, astigmatism and change of path length. Spherical aberration shears into coma and tilt. Pure astigmatism with axes along and perpendicular to the shear direction produces in the shear direction a tilt that can be annulled by a lateral displacement. Astigmatism with axes skew to the shear direction produces, in addition, tilt perpendicular to the shear direction.

If one wavefront is rotated about a principal ray in addition to the lateral shear, then extra information is revealed. For example, with a relative rotation of 180° the comatic errors are doubled. With a rotation through 90° the astigmatic errors are doubled. By inverting one wavefront with respect to the reference wavefront comatic errors and distortion are revealed independent of the effects of change of focus, astigmatism and field curvature.^[49]

Shearing techniques are categorised by the shearing geometry, for example lateral shearing or rotational shearing. The type of beamsplitter involved also categorises the technique, for example whether diffracting or partially reflecting surfaces are used.

Although shear patterns are difficult to interpret, techniques have been developed for calculating the wavefront from the slope data, often called the wavefront difference function.^[50]

Rimmer describes a method for evaluating lateral shear interferograms which reveals errors as small as 0,04 wavelength rms in the measurement of a wavefront with about one wavelength of aberration.^[51]

6.4.2 Advantages and disadvantages of shearing interferometry

Where small shears are involved the intensity profiles are closely matched in both wavefronts, giving good contrast fringes. This is relevant to the asymmetrical intensity distributions that arise from diode laser sources and in particular, from diode laser arrays.

Shearing interferometers can be designed in which the interfering beams travel nearly identical paths. As a result the interferometer has minimal sensitivity to vibration and turbulence, also the temporal coherence requirements are minimised. Limited spatial coherence is required to ensure the sheared wavefronts interfere although the size of the shear is usually kept small.

The major disadvantage is that the fringe patterns are generally not directly related to the wavefront shape as they are when the reference wavefront is flat or spherical. Moreover, the interference pattern does not cover the whole area of the wavefront under test when the shear is large.

With lateral shearing, one interferogram is not sufficient to describe a wavefront unless it has rotational symmetry. Two interferograms must be taken with shears in orthogonal directions and each test must use the same reference wavefront. The amount of shear introduced must be known precisely, requiring the position of points in the wavefront to be identified.

When precise numerical results are required, it is often difficult to interpret the fringes. An exception occurs when the radial shear is large enough for the reference wavefront to be considered virtually error free. This form of radial shear is known as “exploded shear”.

Shearing interferometry is useful for making a null setting where a particular pattern is sought, for example to determine whether a beam is collimated or not.

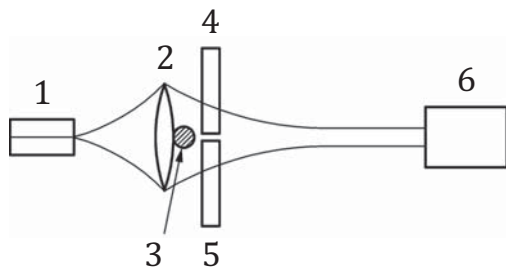
6.4.3 Lateral shearing with a parallel-sided plate

A single plate with near-parallel sides can be used as a beamsplitter for shearing interferometry.^[52] The test wavefront is incident at an inclined angle and the two wavefronts produced, by reflection at the first and second surfaces, overlap with a degree of lateral displacement. The amount of shear can be varied by tilting the plate. If the source coherence is adequate to allow for the difference in optical path lengths, interference patterns are produced by the overlapping wavefronts. To obtain complete information about the wavefront under test, a further orthogonal shear test has to be made.

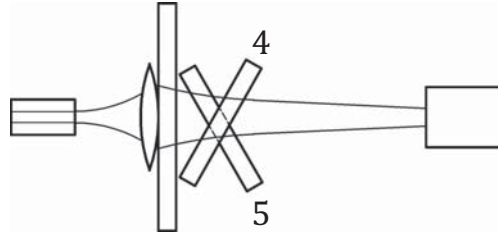
The Jamin interferometer uses two parallel plates in sequence and paths can be chosen that provide equal path lengths for two laterally sheared wavefronts.^[53]

A simple interferometer described by Yaeli has been used to study the near field output from a diode laser array.^[54] Shown in [Figure 8](#), it consists of two adjacent plates placed in the wavefront converging from a lens that is used to form an image of the source at the detector. The wavefront is divided spatially by the plates. The two halves of the converging wavefront are made to overlap and interfere by tilting the two plates in opposite directions, thus shearing the image with itself. A mask is used to prevent stray light from passing through the gap between the two plates. Diffraction at the edges of the mask can be a problem.

The beam envelopes shown in [Figure 8](#) are curved to represent the Gaussian propagation of the laser beam.



a) side view with shear plates aligned



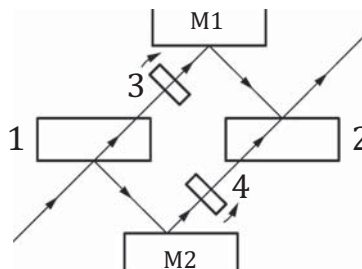
b) plan view with shear plates rotated

Key

- 1 source
- 2 lens
- 3 fine wire
- 4 shear plate
- 5 shear plate
- 6 camera

Figure 8 — Wavefront shearing with two plates**6.4.4 Lateral shear Mach-Zehnder interferometer**

A form of Mach-Zehnder interferometer described by Yaeli and shown in [Figure 9](#) has been used to examine the far-field output of diode arrays with very short coherence lengths.^[54] The incident wavefront is amplitude divided at a beamsplitter. Parallel plates are placed in each arm and are rotated in opposite directions to introduce lateral shear to the wavefronts which are recombined at a second beamsplitter. Compared to the single plate shearing system, the separate paths in the Mach-Zehnder give more control over the shear but the system is less immune to environmental disturbances.

**Key**

- 1, 2 beamsplitters
- 3, 4 shear plates
- M1, M2 interferometer mirrors

Figure 9 — Mach-Zehnder interferometer used for lateral shear study of far-field wavefronts

6.4.5 Radial-shear and exploded shear interferometry

6.4.5.1 General

Radial shear is a form of interferometry in which a wavefront is compared with an expanded image of itself. It is a non-directional technique and as such has advantages over lateral shearing which often requires more than one interferogram to reveal symmetrical aberrations.[55]

Radial shearing is, like lateral shearing, sensitive to wavefront slopes and the interferograms must be interpreted to obtain the true aberration. Hariharan describes a cyclic interferometer for radial shearing.[56] The individual aberrations are reproduced in the interferogram, unchanged except for a scale factor which can be evaluated if the shear ratio is known. Where the wavefront suffers from only one aberration, the interferogram bears a close resemblance to the wavefront profile. The degree of approximation improves as the shear ratio decreases. Where the wavefront suffers from several aberrations the interferogram is more difficult to analyse.

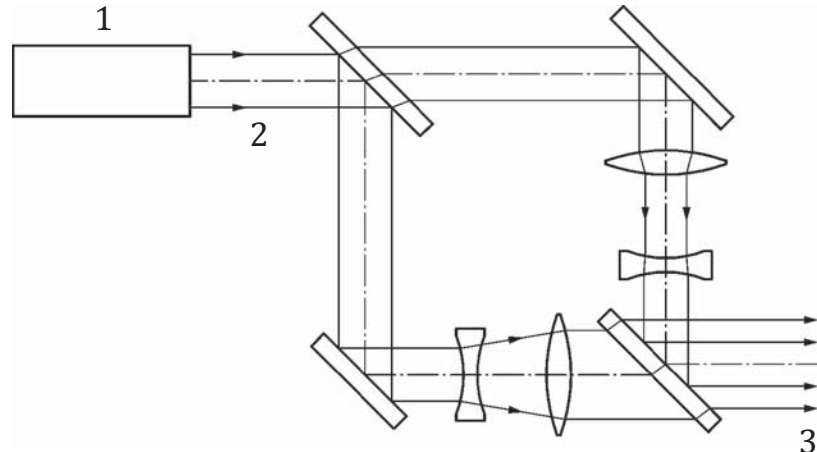
Another form of radial shear is known as “exploded shear”. When the radial expansion is very large, the form of the reference wavefront approaches spherical or flat, and thus the interferogram does not appear in the form of differential slope or slope of the aberrations.

The centre of the test wavefront is usually chosen for expansion as it is usually of higher quality. For example, if the primary aberration is third order spherical, then the magnitude of the aberration varies as the fourth power of the radius from the axis. The aberration over the central 10 % of the wavefront, which is selected for expansion, is 0,01 % of the aberration present over the entire wavefront. Astigmatism over the central 10 % is 1 % of that over the entire wavefront because astigmatism varies as the quadratic power of radius.

6.4.5.2 Exploded (radial) shear Mach-Zehnder

In [Figure 10](#) the radial shear interferometer is based on a Mach-Zehnder design. This requires two beamsplitters and the optical paths are more separated than some other designs. Although this makes the system more sensitive to environmental disturbances it provides more room for optical components. Beam expansion in one arm is achieved with an afocal telescope and it is usual to place a similar but reversed telescope in the other arm to maintain similar optical path lengths.[57]

Once again, it is assumed that the radial shear is large enough to enable a smooth central portion of the wavefront to be selected as reference. The lower energy density in the expanded beam has to be matched by the correct choice of reflectivity at the first beamsplitter.

**Key**

- 1 light source
- 2 nominally collimated beam
- 3 radially sheared wavefronts

Figure 10 — Mach-Zehnder interferometer used for exploded-shear testing

This arrangement has been used to examine wavefronts from sources such as diode lasers. If a lower uncertainty is required then a version with a spatial filter in one arm is used to reduce the errors in the reference wavefront. A disadvantage is that this makes it more difficult to align the source and there is a reduction in the light transmitted.

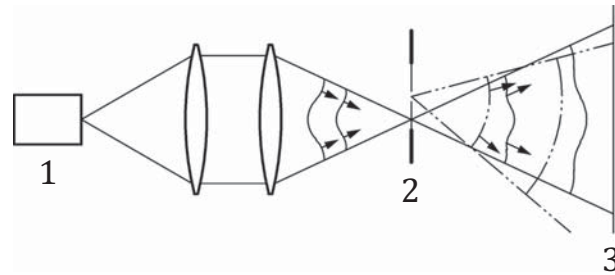
6.5 Point-diffraction interferometers with error-free reference wavefronts

6.5.1 General

These designs use a reference beam that is formed by sampling a part of the test beam with a small aperture and expanding it sufficiently to form what is in effect an error-free reference wavefront.

6.5.2 Point-diffraction interferometer

[Figure 11](#) shows an interferometer design due to Smartt.^[58] The aberrated wavefront is focused to a pinhole aperture formed in a neutral density filter and some of the light in the focused image is diffracted by the pinhole, creating a spherical reference wave. The remainder is transmitted by the neutral density filter surround to the pinhole. The density filter is necessary to attenuate the reference wave to match the lower energy density in the diffracted wavefront. The pinhole diameter is ideally half of the size that the Airy disc would be if the focused beam had no aberration. In one application with a carbon dioxide laser emitting at 10,6 μm , a pinhole of 65 μm was used.^[59]

**Key**

- 1 light source
- 2 pinhole aperture in neutral density filter
- 3 interference pattern on diffusing screen

Figure 11 — Point-diffraction interferometer

Advantages of point diffraction interferometry include the fact that the interference pattern is readily interpreted. The optical paths are closely matched, and this gives reduced sensitivity to environmental disturbances.

A disadvantage is that the best fringe contrast is obtained close to the null setting. Away from the null setting, both transversely and axially, fringe contrast deteriorates. The diffracted wave has a Gaussian intensity profile which may not match the profile of the test beam. Attention must be paid to the quality of the lenses that are used to focus the beam to the pinhole as they may introduce additional aberration.

As with many other systems when used with diode lasers, care has to be taken to avoid back reflections from the coupling optics giving rise to mode instabilities causing the output to hop between longitudinal modes.[\[60\]](#)

Phase modulation is difficult to achieve although not impossible.[\[61\]](#) The pinhole can be formed in a piece of birefringent material such as mica, selected such that it acts as a half-wave plate and oriented so as to rotate the direction of polarization of the incident light by 90°. The diffracted spherical wave and directly transmitted wave then have orthogonal polarisations. An electro-optic modulator is used to shift the relative phases of the beams.

A point diffraction interferometer using a reflective pinhole and employing a delay line for phase-shifting was proposed by Sommargren and used for precision wavefront measurement.[\[62\]](#)

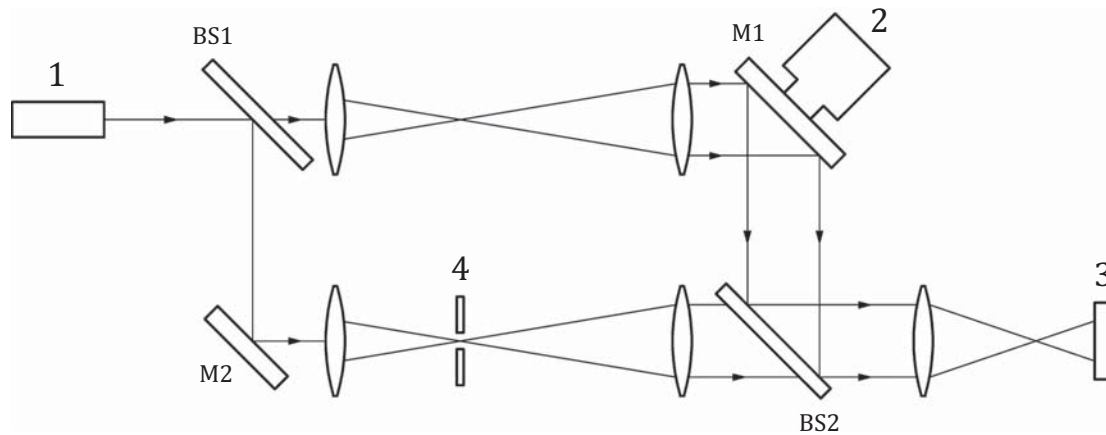
6.5.3 Mach-Zehnder interferometer with spatial filter

This is a cross between the radial-shear Mach-Zehnder and Smartt point diffraction interferometers. [Figure 12](#) shows an equal-path Mach-Zehnder where a reference wavefront is generated by focusing the beam in one arm to a small aperture.[\[63\]](#) The illumination selected by the aperture expands to form a spherical wavefront which is then collimated and combined with the test beam. The pinhole diameter is ideally 0,5 times the size of the Airy disc.

High quality optical components operating at low numerical aperture ratios are used. A pair of lenses is used to focus the reference beam to the spatial filter and recollimate it. The optical path length introduced by these lenses can be matched by inserting a similar pair in the test arm. Care has to be taken to ensure these lenses are of high quality.

The interference patterns are easy to interpret and separate reference and test beam paths give easy access for control, such as beam intensity ratio, path length adjustment and modulation.

Disadvantages include the large number of optical components involved, difficulty in alignment and optical paths that are separated, giving sensitivity to environmental disturbances. The diffracted wave has a Gaussian profile which may not match that of the test wavefront, but probably gives a better match than a uniform profile would.

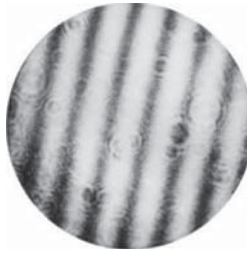


Key

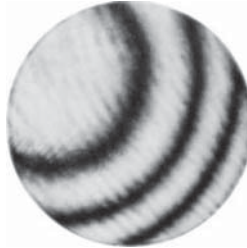
1	light source
2	mirror on PZT mount
3	detector array
4	spatial filter
M1 and M2	interferometer mirrors
BS 1 and BS 2	beamsplitters

Figure 12 — Mach-Zehnder interferometer with spatially-filtered reference arm

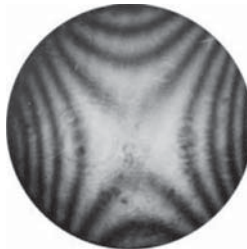
[Figure 13](#) shows wavefront interferograms produced with an interferometer following the design shown in [Figure 12](#). In records a) to c) the source was a beam from a helium-neon laser expanded to 6 mm diameter. In record d) the source was a laser diode fitted with a collimating lens. The diameter of the spatial filter in the reference arm was 5 μm .



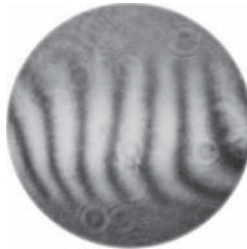
a)



b)



c)



d)

Key

- a) tilt fringes
- b) defocus with tilt
- c) astigmatism introduced by inserting $-0,75$ D cylinder lens test wavefront
- d) output from a laser diode

Figure 13 — Mach-Zehnder interferograms, using a spatially-filtered reference arm

6.6 Lateral shearing and the Ronchi test

The Ronchi test is attributed to Vasco Ronchi in 1923 and he gives a review of its development over the years.^[64] It is very simple to perform and is widely used to give an indication of the quality of optical components such as concave mirrors. To test a concave mirror, a coarse grating with dark and clear bands

is placed near the centre of curvature of a mirror. For a geometrical optics based explanation consider an image of the grating to be formed superimposed on the grating. This generates moire patterns and their shapes give an indication of the aberrations of the mirror. The test gives a direct measure of the transverse aberrations.

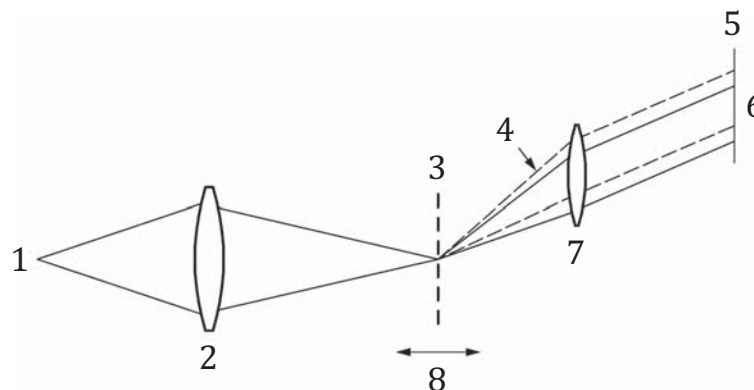
Another explanation is that the Ronchi grating acts as a diffraction grating, producing in many orders a series of laterally sheared images of the pupil which interfere to produce the fringe pattern. As well as gratings with straight equally spaced bands, Ronchi gratings can take other forms. For example, radial gratings are sometimes used.

The simple Ronchi test is mostly used for qualitative measurements as the patterns can be difficult to interpret in the presence of complex aberrations.

6.7 Lateral shearing with a double frequency grating

With the Ronchi test, unless the shear is at least one half the pupil diameter, more than two beams overlap and may cause unnecessary interference. A technique described by Wyant is similar to the Ronchi test but is claimed to be easier to align. Outlined in [Figure 14](#) it uses a single component, a double-frequency diffraction grating, as a beamsplitter.

By choosing the frequencies of the grating to suit specific diffraction angles the interferometer can be made to produce any desired amount of shear and still have only two-beam interference.^[65] The two interfering beams always have the same intensity and thus very good contrast fringes can be obtained. By making the grating with crossed features, shear in two orthogonal directions is obtained simultaneously.



Key

- 1 point source
- 2 lens under test
- 3 double frequency grating
- 4 two sets of diffracted rays
- 5, 6 sheared images of exit pupil of system under test
- 7 imaging lens
- 8 axial adjustment for grating

Figure 14 — Double frequency grating used for lateral shear

7 Summary of wavefront sensing methods

Tables 1, 2 and 3 enable the characteristics of different wavefront sensing methods to be readily compared.

Table 1 — Wavefront sensing methods and characteristics: Tests

	Knife-edge test	Hartmann screen test	Shack-Hartmann test	Ronchi test
Method outlined	Beam focused to knife edge which blocks portions of wavefront.	Opaque screen with array of small apertures samples wavefront on a regular grid. Direction of beamlets determined by measuring intersection of beamlets with another plane.	Lenslet array generates array of spots from test wavefront. The transverse positions of the spots relate to the local slopes of the wavefront and the form of the wavefront is calculated.	Wavefront deduced from "Ronchigrams" formed by superposition of image of a coarse grating on the grating. Explained with both geometrical and interference models. Is a form of shearing interferometry.
Common uses	Testing mirrors and lens systems.	Testing mirrors and lens systems.	Measuring wavefronts from sources and components.	Testing mirrors and lens systems.
Advantages	Simple sensitive test. Useful for null testing and measurement of zonal errors in near-spherical wavefronts.	Wide dynamic range. Reasonable optical efficiency.	High dynamic range, white light capability. Lower sensitivity to vibration than, for example, interferometry. Optically efficient.	Simple test gives a quick indication.
Disadvantages	Heights deduced from slopes. Accurate knowledge of knife edge position required. Difficult to test aspheric wavefronts.	Samples wavefront at discrete points. Historically used photographic records which take a finite time to process. To sample a small area requires small holes in the mask which give unwanted diffraction effects.	Careful alignment and calibration is necessary for accurate use.	Complex aberrations difficult to interpret.
Wavelength dependence	Minimal.	None.	Wavelength range limited by chromatic aberration of microlens array and detector efficiency.	Works with white light.
Coherence requirements	Minimal.	Partial coherence.	Coherence only required over microlens aperture.	Point source required.

Table 2 — Wavefront sensing methods and characteristics: Shearing interferometry

Shearing interferometry			
Method outlined	Intensity pattern formed by interference with a reference wavefront reveals phase distribution. The reference may be a copy of the test wavefront or a perfect spherical wavefront derived from the test wavefront, superimposed with a known shear.		
Types of shear	Lateral shear	Radial shear	Point diffraction interferometer
Optical path design	Based on parallel plate, Michelson or Mach-Zehnder or interferometers. Interfering wavefronts displaced laterally by relative tilt.	Based on Mach-Zehnder or Michelson interferometer. Interfering wavefronts magnified by differing amounts by optical design.	Wavefront focused to pinhole which generates spherical reference wave to interfere with test wavefront. Test wavefront transmitted with reduced intensity to match reference wavefront.
Beamsplitting method	Amplitude division.	Amplitude division.	Spatial division – small aperture in neural density filter often used.
Common uses	Wavefront measurement and testing optical components		
Advantages	Wavefront deduced from interferogram.	Efficient use of light. One interferogram provides information for all directions. For large shear, wavefront deformations are directly represented.	Small size. Common-path design minimises sensitivity to environmental disturbances. Clear indication of aberrations.
Disadvantages	Michelson arrangement only allows for shear in one direction. Mach-Zehnder may be adjusted to give shear in two directions. Non-common path interferometers may be sensitive to environmental disturbances.	Attenuation of one wavefront necessary to obtain good contrast where large shear values are involved.	Inefficient use of light. Test wavefront attenuation is necessary to obtain optimum contrast in interference pattern. Aperture size must be carefully chosen. Difficult to apply phase shifting techniques to analyse wavefront.
Wavelength dependence	Interferometry is wavelength dependent although examples of the shearing interferometer have been designed for white light use.		Optimum size of pinholes is a function of wavelength.
Coherence requirements	Coherence required.		Spatial coherence required.

Table 3 — Wavefront sensing methods and characteristics: Sensing

	Curvature sensing	Phase diversity sensing
Method outlined	Uses two image detectors to detect the irradiance distribution either side of the wavefront focus.	Wavefront phase is retrieved from two intensity images symmetrically placed about wavefront under test. Use phase diversity in wavefront test for non- focusing beam.
Common uses	Measuring focused wavefronts. Particular applications with adaptive optics.	Measuring wavefronts from sources and components.
Advantages	Small size, simple construction. Compared with the Shack-Hartmann sensor, the number of pixels required is reduced, enabling smaller, low-cost sensor.	Light weight, robust, compact design.
Disadvantages	Dynamic range limited by magnitude of optical aberrations.	Dynamic range limited.
Wavelength dependence	White light.	White light in general. Monochromatic for system with gratings.
Coherence requirements	Accepts broad band source.	Minimal.

Bibliography

- [1] ISO 10110-5, *Optics and photonics — Preparation of drawings for optical elements and systems — Part 5: Surface form tolerances*
- [2] ISO 10110-14, *Optics and photonics — Preparation of drawings for optical elements and systems — Part 14: Wavefront deformation tolerance*
- [3] ISO/TR 14999-1, *Optics and photonics — Interferometric measurement of optical elements and optical systems — Part 1: Terms, definitions and fundamental relationships*
- [4] ISO/TR 14999-2, *Optics and photonics — Interferometric measurement of optical elements and optical systems — Part 2: Measurement and evaluation techniques*
- [5] ISO/TR 14999-3, *Optics and photonics — Interferometric measurement of optical elements and optical systems — Part 3: Calibration and validation of interferometric test equipment and measurements*
- [6] ISO 15367-2, *Lasers and laser-related equipment — Test methods for determination of the shape of a laser beam wavefront — Part 2: Shack-Hartmann sensors*
- [7] GEARY J.M. *Wavefront sensors*. SPIE Optical Engineering Press vol TT18, 1995
- [8] HARIHARAN P. *Optical Interferometry*. Academic Press Elsevier Science, 2003
- [9] MANSURIPUR M. *Classical Optics and its applications*. Cambridge University Press, 2002
- [10] MALACARA D. *Optical shop testing*. John Wiley and Sons, 2007
- [11] TEAGUE M.R. Image formation in terms of the transport equation. *J. Opt. Soc. Am.* 1985, **2** (11) pp. 2019–2026
- [12] FOUCAULT L.M. Description des Procèdes Employes pour Reconnaître la Configuration des Surfaces Optiques. *E.R. Acad. Sci.* 1858, **47** p. 958
- [13] FIRESTER A., HELLER M., SHENG P. Knife-edge scanning measurements of subwavelength focused light beams. *Appl. Opt.* 1977, **16** (7) pp. 1971–1974
- [14] ARNAUD J.A. et al. Technique for fast measurement of gaussian laser beam parameters. *Appl. Opt.* 1971, **10** (12) pp. 2775–2776
- [15] SUZAKI Y., & TACHIBANA A. Measurement of the μm sized radius of Gaussian laser beam using the scanning knife-edge. *Appl. Opt.* 1975, **14** (12) pp. 2809–2810
- [16] SUZAKI Y., & TACHIBANA A. Measurement of the Gaussian laser beam divergence. *Appl. Opt.* 1977, **16** (6) pp. 1481–1482
- [17] GAVIOLA E. On the quantitative use of the Foucault knife-edge test. *J. Opt. Soc. Am.* 1936, **26** p. 163
- [18] PLATZECK R., & GAVIOLA E. On the errors of testing and a new method of surveying optical surfaces and systems. *J. Opt. Soc. Am.* 1939, **29** pp. 484–500
- [19] ESCOBAR S.R. Adjustable magnification anamorphic beam expander. Report UCRL-10-106488, Lawrence Livermore National Laboratory (1990)
- [20] SNYDER J. J., & CABLE A. E. Cylindrical lenses improve laser diode beams. *Laser Focus World*, 97-100 (Feb 1993)
- [21] PELED S. Near- and far-field characterization of diode lasers. *Appl. Opt.* 1980, **19** (2) pp. 324–328

- [22] RAGAZZONI R. Pupil plane wavefront sensing with an oscillating prism. *J. Mod. Opt.* 1996, **43** pp. 289–293
- [23] RICCARDI A., BINDI N., RAGAZZONI R., ESPOSITO S., STEFANINI P. “Laboratory characterisation of a Foucault-like wavefront sensor for adaptive optics.” Adaptive Optical System Technologies, R K Tyson ed. *Proc. SPIE*. 1998, **3353** pp. 941–951
- [24] BURVALL A., DALY E., CHAMOT S.R., DAINTY C. Linearity of the pyramid wavefront sensor. *Opt. Express*. 2006 December, **14** (25) pp. 11925–11934
- [25] HARTMANN J. Objectivuntersuchungen. *Zt. Instrumentenk.* 1904, **24** p. 1
- [26] LOIBL B. Hartmann tests on large telescopes carried out with a small screen in a pupil plane. *Astron. Astrophys.* 1980, **91** pp. 265–268
- [27] KINGS LAKE R. The measurement of the aberrations of a microscope objective. *J. Opt. Soc. Am.* 1936, **26** pp. 251–256
- [28] BAKER L.R., & WHYTE J.N. New instrument for assessing lens quality by pupil scanning (spot diagram generation) Japanese Journal of Applied Physics, vol 4, supplement 1, 1965 – Proceedings of the Conference on Photographic and Spectroscopic Optics 1964
- [29] WILLIAMS T. A spot diagram generator for lens testing. *Opt. Acta (Lond.)*. 1968, **15** (6) pp. 553–556
- [30] BAKER L.R., & WILLIAMS T.L. New electronic wavefront plotter. *Appl. Opt.* 1965, **4** (3) pp. 285–287
- [31] WILLIAMS T.L. A pupil-scan aberration analyser. *Optica Acta*, vol. 20 no. 3, pp 1972
- [32] PLATT B.C., & SHACK R. History and principles of Shack-Hartmann wavefront sensing. *J. Refract. Surg.* 2001 Sept/Oct, **17** pp. S573–S577
- [33] SHACK R.V., & PLATT B.C. Use of a lenticular Hartmann screen. *J. Opt. Soc. Am.* 1971, **61** p. 656
- [34] SOUTHWELL W.H. Wave-front estimation from wave-front slope measurements. *J. Opt. Soc. Am.* 1980, **70** (8) pp. 998–1006
- [35] BELOUSOVA I.M. et al. Wavefront analyzers of adaptive optical systems. *Sov. J. Opt. Tech.* 1992, **59** (6) pp. 341–351
- [36] MICHAU V. et al. Hartmann-Shack wavefront sensor for laser diode testing. Proc SPIE Int. conf. on Optical Science and Engineering, Paris, 1989
- [37] KNOX S.D., HALL R.G., STEVENS R.F. Traceable astigmatism measurements with wavefront sensors. Proc. of 6th Int. workshop, Adaptive Optics for Industry and Medicine, National University of Ireland. Edited by Chris Dainty, Imperial College Press, 2008
- [38] RODDIER F. Curvature sensing and compensation: a new concept in adaptive optics. *Appl. Opt.* 1988, **27** (7) pp. 1223–1225
- [39] BLANCHARD P.M., & GREENAWAY A H. Simultaneous multiplane imaging with a distorted diffraction grating. *Appl. Opt.* 1999, **38** (32) pp. 6692–6699
- [40] BLANCHARD P.M. et al. Phase-diversity wave-front sensing with a distorted diffraction grating. *Appl. Opt.* 2000, **39** (35) pp. 6649–6655
- [41] GONSALVES R.A. Phase retrieval and diversity in adaptive optics. *Opt. Eng.* 1982, **21** p. 829
- [42] GERCHBERG R.W., & SAXTON W.O. A practical algorithm for the determination of phase from image and diffraction plane pictures. *Optik (Stuttg.)*. 1972, **35** pp. 237–246
- [43] WOODS S.C., & GREENAWAY A.H. Wave-front sensing by use of a Green’s function solution to the intensity transport equation. *J. Opt. Soc. Am. A Opt. Image Sci. Vis.* 2003, **20** pp. 508–512

- [44] HALL S.R.G., ROBINSON D., KNOX S.D., YANG H., SCOTT A.M., WOODS S.C. et al. Improvement and commissioning of a novel technology for the measurement of laser-beam profiles. Proc. SPIE Photonics West, Laser Resonators and Beam Control IX. Alexis V. Kudryashov, Alan H. Paxton, Vladimir S. Ilchenko. San Jose, CA. *Proc. SPIE*. 2007, **6452** p. 645208
- [45] BATES W.J. A wavefront shearing interferometer. *Proc. Phys. Soc.* 1947, **59** pp. 940–950
- [46] SAUNDERS J.B. Inverting Interferometer. *J. Opt. Soc. Am.* 1955, **45** p. 133
- [47] BROWN D.S. *Proc. Phys. Soc. B.* 1959, **67** p. 232
- [48] Birch K.G. Green F.J. Interferometric testing of aspheric surfaces. NPL report OM12 (Feb 1972)
- [49] GATES J.W. The measurement of comatic aberrations by interferometry. *Proc. Phys. Soc. B.* 1955, **68** p. 1065
- [50] WYANT J.C. Use of an ac heterodyne lateral shear interferometer with real-time wavefront correction systems. *Appl. Opt.* 1975, **14** (11) pp. 2622–2626
- [51] RIMMER M.P. Method for evaluating lateral shearing interferograms. *Appl. Opt.* 1974, **13** (3) pp. 623–629
- [52] MURTY M.V.R.K. The use of a single plane parallel plate as a lateral shearing interferometer with a visible gas laser source. *Appl. Opt.* 1964, **3** (4) pp. 531–534
- [53] MURTY M.V.R.K. Some modifications of the Jamin interferometer useful in optical testing. *Appl. Opt.* 1964, **3** (4) pp. 535–538
- [54] YAELI J. Phase measurement of laser diode array radiation. *Appl. Phys. Lett.* 1986, **49** (8) pp. 427–429
- [55] BROWN D.S. Radial shear interferometry. *J. Sci. Instrum.* 1962, **39** pp. 71–72
- [56] HARIHARAN P. Radial shearing interferometry. *J. Sci. Instrum.* 1961, **38** pp. 428–432
- [57] LANGE S.R. Self-referencing wavefront interferometer for laser sources. *SPIE*. 1985, **551** pp. 6–11
- [58] SMARTT R.N., & STRONG J.J. *Opt. Soc. Am.* 1972, **62** p. 737
- [59] KOLIOPOULOS C. et al. Infrared point-diffraction interferometer. *Opt. Lett.* 1978, **3** (3) pp. 118–120
- [60] CREATH K. Interferometric investigation of a diode laser source. *Appl. Opt.* 1985, **24** (9) pp. 1291–1293
- [61] WYANT J. Phase measurement systems for adaptive optics *Agard Conf Proc* pt 300 48-1 48-12 (1981)
- [62] SOMMARGREN G.E. et al. 100-picometer interferometry for EUVL. *Proc. SPIE*. 2002, **4688** pp. 316–328
- [63] COCHRAN E.R. Design and evaluation of laser sources with high-quality wavefronts. *Appl. Opt.* 1991, **30** (34) pp. 5037–5048
- [64] RONCHI V. Forty years of history of a grating interferometer. *Appl. Opt.* 1964, **3** (4) pp. 437–451
- [65] WYANT J.C. Double frequency grating lateral shear interferometer. *Appl. Opt.* 1973, **12** (9) pp. 2057–2059
- [66] ISO 10110-8, *Optics and photonics — Preparation of drawings for optical elements and systems — Part 8: Surface texture; roughness and waviness*
- [67] ISO 10110-12, *Optics and photonics — Preparation of drawings for optical elements and systems — Part 12: Aspheric surfaces*

ICS 37.020

Price based on 27 pages